

## Research Paper

# Short-Wave Infrared Reflectance Investigation of Sites of Paleobiological Interest: Applications for Mars Exploration

ADRIAN BROWN,<sup>1</sup> MALCOLM WALTER,<sup>1</sup> and THOMAS CUDAHY<sup>1,2</sup>

### ABSTRACT

Rover missions to the rocky bodies of the Solar System and especially to Mars require light-weight, portable instruments that use minimal power, require no sample preparation, and provide suitably diagnostic mineralogical information to an Earth-based exploration team. Short-wave infrared (SWIR) spectroscopic instruments such as the Portable Infrared Mineral Analyser (PIMA, Integrated Spectronics Pty Ltd., Baulkham Hills, NSW, Australia) fulfill all these requirements. We describe an investigation of a possible Mars analogue site using a PIMA instrument. A survey was carried out on the Strelley Pool Chert, an outcrop of stromatolitic, silicified Archean carbonate and clastic succession in the Pilbara Craton, interpreted as being modified by hydrothermal processes. The results of this study demonstrate the capability of SWIR techniques to add significantly to the geological interpretation of such hydrothermally altered outcrops. Minerals identified include dolomite, white micas such as illite-muscovite, and chlorite. In addition, the detection of pyrophyllite in a bleached and altered unit directly beneath the succession suggests acidic, sulfur-rich hydrothermal activity may have interacted with the silicified sediments of the Strelley Pool Chert. **Key Words:** Pilbara—Short-wave infrared spectroscopy—Mars—Stromatolites—Archean. *Astrobiology* 4, 359–376.

### INTRODUCTION

**S**HORT-WAVE INFRARED (SWIR) reflectance spectroscopy has gained recognition in the exploration and mining community due to its speed, simplicity, and ability to characterize alteration zones around ore bodies. Recent SWIR studies (Huston *et al.*, 1999; Thompson *et al.*, 1999; Yang *et al.*, 2000, 2001; Herrmann *et al.*, 2001; Bierwirth *et al.*, 2002; Thomas and Walter, 2002) have em-

phasized the instrument's ability to detect alteration minerals such as white micas and chlorites. Each of these studies was conducted using the Australian-built Portable Infrared Mineral Analyser (PIMA) instrument.

SWIR spectroscopy instruments have been suggested as an instrument for use on future landed missions to Mars (see, *e.g.*, Blaney, 2002). To test the SWIR technique in a geologic setting comparable to the ancient flood basalts of Mars,

---

<sup>1</sup>Australian Centre for Astrobiology, Macquarie University, North Ryde, New South Wales, Australia.

<sup>2</sup>CSIRO Division of Exploration and Mining, ARRC Centre, Technology Park, Western Australia, Australia.

fieldwork was undertaken in the arid, 3.5-Ga Pilbara Craton of Western Australia. Over 250 SWIR spectra were obtained by a hand-held PIMA II spectrometer at an outcrop of a heavily silicified, stromatolitic Archean carbonate-chert succession to simulate the investigation of such an outcrop by a rover on Mars.

To simulate the rover responding to commands from an Earth-based exploration team, spectra were taken only on accessible weathered surfaces of the outcrop, and care was taken to target mineral assemblages that could be distinguished visually. This simulated a situation whereby a remote command team would possess only panoramic color images from the rover to select locations for collection of spectra.

### GEOLOGICAL SETTING

The North Pole Dome in the East Pilbara Granite Greenstone Terrane (Van Kranendonk, 2000) is a structural dome of bedded, dominantly mafic greenstone sequences (the Warrawoona Group) that dip gently away from a central monzogranite. The monzogranite has been interpreted as a syn-volcanic laccolith, a product of diapiric uprise and consanguineous magmatism (Van Kranendonk, 2000), though this hypothesis has recently been challenged because of a gravimetric survey that suggests the granite may be a shallow feature underlain by basaltic material (Blewett *et al.*, 2004). Minor occurrences of felsic volcanic rocks interbedded with the greenstones are capped by cherts that indicate hiatuses in volcanism (Van Kranendonk, 2000).

The dating of a stratigraphic column of the Warrawoona Group is presented in Table 1. Stromato-

lite and putative microfossil occurrences have been documented within the Warrawoona Group at three distinct stratigraphic levels—within the Dresser Formation, Apex Chert, and Strelley Pool Chert (Dunlop *et al.*, 1978; Walter *et al.*, 1980; Awramik *et al.*, 1983; Lowe, 1983; Schopf, 1993; Ueno, 1998; Hofmann *et al.*, 1999; Van Kranendonk, 2000; Ueno *et al.*, 2001a,b; Van Kranendonk *et al.*, 2003). The North Pole Dome is interpreted as an early setting for life (Groves *et al.*, 1981; Buick, 1990).

The rocks of the Warrawoona Group are dominated by tholeiitic and komatiitic volcanic successions, which have been suggested as an analogue for the flood basalts of Mars (Baird *et al.*, 1981; Reyes and Christensen, 1994; Mustard and Sunshine, 1995; Christensen *et al.*, 2000). Although the Earth and Mars have experienced vastly different weathering environments in the past 3.5 billion years, the ancient age of the Archean rocks of the North Pole Dome makes them a compelling analogue for similarly aged parts of the southern highlands on Mars. The preservation state of the Warrawoona group is generally excellent, in contrast with other Early Archaean terranes. Metamorphism has not exceeded greenschist facies throughout the North Pole Dome, and is most commonly at prehnite-pumpellyite facies (Van Kranendonk, 2000). The presence of putative microfossils and stromatolites at the North Pole Dome makes it an ideal test bed for astrobiological techniques designed to examine ancient fossilized life.

A number of contributions have been made regarding the depositional setting of the Warrawoona Group. Some researchers have suggested a shallow marine environment based on the presence of pillow basalts, sedimentary analysis, and Rare Earth Element (REE) systematics (Buick and

TABLE 1. STRATIGRAPHIC COLUMN OF WARRAWOONA GROUP UNITS PRESENT AT THE NORTH POLE DOME (VAN KRANENDONK, 2000)

<i>Age (Ga)</i>	<i>Unit</i>	<i>Fossil assemblages</i>
3.458	Euro Basalt Strelley Pool Chert Panorama Formation	Well-preserved conical stromatolites (Hofmann <i>et al.</i> , 1999)
3.470	Apex Basalt Duffer Formation Dresser Formation	Microfossils within Apex Chert (Schopf, 1993)
3.515	Mt. Ada Basalt Coonterunah Group	Domical stromatolites and microfossils (Walter <i>et al.</i> , 1980; Awramik <i>et al.</i> , 1983)

Dates are derived from U-Pb isotopes from zircons in the units and are accurate to approximately 3 million years from Thorpe (1992).

Dunlop, 1990; Van Kranendonk *et al.*, 2003), whereas others have suggested an Archean mid-ocean ridge setting due to geochemical analysis of basaltic successions and apparent similarities between hydrothermal alteration patterns at the North Pole Dome and in modern mid-ocean ridge deposits (Kitajima *et al.*, 2001). The most recent interpretations invoke a caldera-like environment on an oceanic plateau based upon interpretation of volcanic conduits in the north of the North Pole Dome (Van Kranendonk and Pirajno, 2004).

Barley (1984) suggested that silicification and carbonate-chlorite alteration of North Pole Dome greenstones were the result of low temperature, low pressure (“epithermal”) hydrothermal alteration. Silicification associated with epithermal systems in early Archean greenstone terrains is almost ubiquitous (De Wit *et al.*, 1982; Gibson *et al.*, 1983). Others have concluded that silicification in the Dresser Formation and Strelley Pool Chert occurred very early after the deposition of a shallow subaqueous to subaerial evaporite sequence (Lowe, 1983; Buick and Dunlop, 1990). The process of early silicification is critically important for preservation of delicate biogenic structures such as microbial mats.

The Trendall Locality, within the Strelley Pool Chert in the southwest part of the North Pole Dome, contains a silicified carbonate-clastic succession with well-preserved stromatolites (Hofmann *et al.*, 1999). The origin of these stromatolites is controversial because of their ancient age and apparent lack of preserved microfossils. The three-dimensional conical morphology of the laminae and REE analysis suggesting deposition in Archean seawater conditions support a biotic origin during normal marine stromatolite precipitation (see, *e.g.*, Fig. 3g) (Hofmann *et al.*, 1999; Van Kranendonk *et al.*, 2003). However, Lindsay *et al.* (2003) have proposed the structures formed abiotically by direct carbonate precipitation from sub-seafloor syn-depositional hydrothermal activity. They propose that evidence from cavity filling textures suggest CO<sub>2</sub>-rich hydrothermal fluids were responsible for deposition of dolomite, with no biotic mediation, and later silicification took place as the hydrothermal activity waned.

In any case, it is clear that the Trendall locality has been affected by hydrothermal activity, either by syn-depositional activity, post-depositional activity, or both processes. We adopt the view that hydrothermal alteration mediated the deposition of at least some parts of the Strelley Pool Chert.

## METHODOLOGY

Reflectance spectroscopy utilizing the SWIR region of the electromagnetic spectrum (1.3–2.5  $\mu\text{m}$ ) often exploits absorption bands due to bonds between hydroxyl (OH<sup>-</sup>) ions and nearby cations in the crystal lattice. Minerals that contain hydroxyl ions are commonly associated with hydrothermal alteration zones that formed when hot (>50°C) water entraining solutes passed through rock pores or fissures.

Figure 1 displays the SWIR spectra of several alteration minerals typical of hydrothermal systems. The absorption bands around 2.2  $\mu\text{m}$  are caused by a combination of the  $\nu_2$  fundamental stretching vibration mode of the OH<sup>-</sup> hydroxyl ion with the Al-OH bending mode in the crystal lattice of each mineral (Hunt, 1979). The central wavelength of the absorption band varies slightly because of the type of cation (for example, Fe<sup>2+</sup> or Mg substituting for Al) ionically bonded to the hydroxyl ion. This spectral characteristic allows the determina-

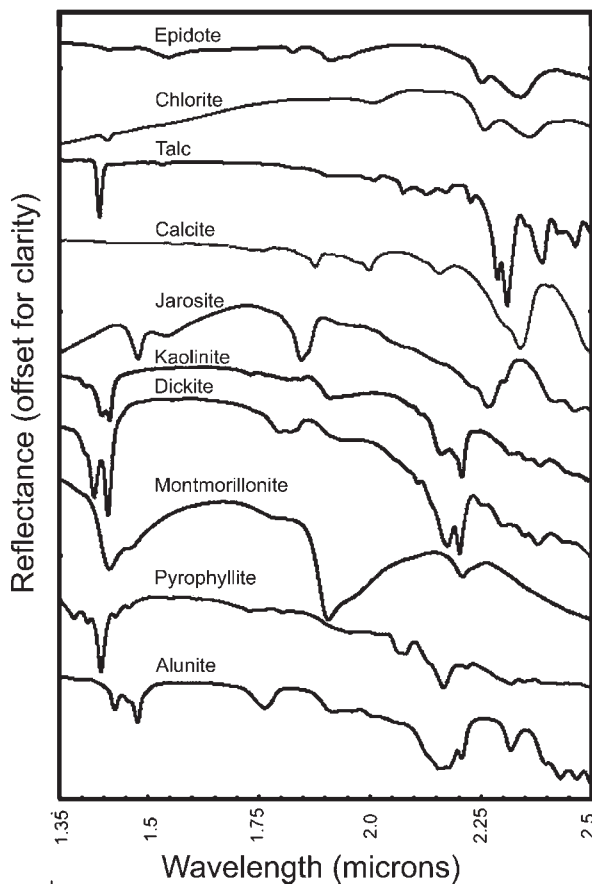


FIG. 1. SWIR spectra of common alteration minerals. Courtesy of ISPL (<http://www.intspec.com>).

tion of relative proportions of Mg or Fe<sup>2+</sup> to Al in white micas like muscovite-phengite. Another significant absorption band in the SWIR region is the carbonate (CO<sub>3</sub><sup>2-</sup>) vibration mode at 2.32 μm, the position of which also shifts wavelength with varying amounts of Ca and Fe<sup>2+</sup> relative to Mg in magnesite, dolomite, and calcite (Gaffey, 1986).

Table 2 gives a partial list of alteration minerals discernible using SWIR spectra, as well as details regarding their common mode of occurrence (Thompson *et al.*, 1999).

Mapping alteration systems surrounding ore bodies has long been a pursuit of economic geologists (Meyer and Hemley, 1967). By recognizing distinctive mineralogies that typically form zones within hydrothermal alteration systems, suitable "vectors to ore" can be determined (Galley, 1993). For example, the presence of white mica or sericite is often the result of the breakdown of plagioclase when an igneous rock is hydrothermally altered. By mapping the occurrence of white mica, the direction of flow in hydrothermal veins or alteration zones can be delineated. Airborne SWIR studies are a particularly effective tool for regional mapping of white mica or sericite veins (Cudahy *et al.*, 2000; Brown, 2003), and correlation on the ground is possible using hand-held or rover-mounted instruments such as the PIMA.

The PIMA instrument measures reflected light from an internal light source at SWIR wavelengths between 1.3 and 2.5 μm. The instrument must be in direct contact with the sample during analysis, since it uses an internal light source for

illumination. This configuration makes it an ideal instrument for analyzing outcrop surfaces (as in this study), rock chips, or crushed powders. The instrument integrates the reflected light from a small region of approximately 10 mm in diameter in front of the detector.

The spectral resolution of the PIMA is 7–10 nm, and the spectral sampling interval is 2 nm. The unit has a signal-to-noise ratio of between 3,500 and 4,500 to 1 (see <http://www.intspec.com>). Measurements typically take 1–2 min to acquire, depending on the selected integration time. Following each spectrum collection cycle, the instrument automatically carries out a reflection calibration against a known internal standard contained within the PIMA. Wavelength calibration is carried out periodically by comparing the spectrum of the internal standard with a known baseline spectrum provided by the manufacturer. The instrument operates from a 12-V NiCd battery. Internal temperature and battery status are measured and reported to an attached WinCE palm computer or laptop PC. Spectra from the PIMA instrument can be downloaded for further analysis using programs such as Microsoft Excel or The Spectral Analyst (TSA).

PIMA instruments have been manufactured by Integrated Spectronics Pty Ltd. (Baulkham Hills, NSW, Australia) since 1991. Approximately 250 units are in service throughout the world. Two models were produced: the PIMA II and the upgraded PIMA SP model. Further PIMA models are under development (T. Cocks, personal communication).

TABLE 2. PARTIAL LIST OF MINERALS DETECTABLE USING SWIR INSTRUMENTS

<i>Mineral</i>	<i>Standard formula</i>	<i>Example mode of occurrence</i>
Chlorite	(Mg,Al,Fe) <sub>12</sub> [(Si,Al) <sub>8</sub> O <sub>20</sub> ](OH) <sub>16</sub>	Diagenesis, metamorphism, and hydrothermal alteration
Illite-muscovite	K <sub>2</sub> Al <sub>4</sub> (Si <sub>6</sub> Al <sub>2</sub> )O <sub>20</sub> (OH) <sub>4</sub>	Diagenesis, metamorphism, and hydrothermal alteration
Pyrophyllite	Al <sub>2</sub> Si <sub>4</sub> O <sub>10</sub> (OH) <sub>2</sub>	Diagenesis and hydrothermal alteration
Saponite	(Ca,Na) <sub>0.67</sub> (Mg,Fe) <sub>6</sub> (Si,Al) <sub>8</sub> O <sub>20</sub> (OH) <sub>4</sub> · 8H <sub>2</sub> O	Weathering, sedimentary, and hydrothermal alteration
Calcite	CaCO <sub>3</sub>	Ca-rich hydrothermal alteration and marine sedimentary
Dolomite	CaMg(CO <sub>3</sub> ) <sub>2</sub>	Mg alteration and diagenesis
Gypsum	CaSO <sub>4</sub> · 2H <sub>2</sub> O	Evaporite
Epidote	Ca <sub>2</sub> Fe <sup>3+</sup> Al <sub>2</sub> Si <sub>3</sub> O <sub>12</sub> (OH)	Ca-rich hydrothermal alteration
Serpentine	Mg <sub>3</sub> Si <sub>2</sub> O <sub>5</sub> (OH) <sub>4</sub>	Alteration of ultramafic rocks
Talc	Mg <sub>3</sub> (Si <sub>4</sub> O <sub>10</sub> )(OH) <sub>2</sub>	Alteration of ultramafic and carbonate rocks
Jarosite	KFe <sub>3</sub> (SO <sub>4</sub> ) <sub>2</sub> (OH) <sub>6</sub>	Weathering of Fe sulfide-bearing rocks

The standard formula is from Deer *et al.* (1992). Example mode of occurrence is modified from that of Thompson and Thompson (1996).

In this study, the TSA version 4 program was used to automatically identify the minerals in the acquired SWIR spectra based on a comparison of the acquired spectrum to a library of pure end-member spectra. TSA uses a proprietary algorithm developed at CSIRO to identify the predominant one or two SWIR-active minerals within the sample. If the spectrum lacks sufficient infrared-active features to identify the phase(s), the rock is declared “aspectral.” This automated identification procedure simulates a scenario where a rover independently determines the minerals present in a rock at a landing site and reports the results of its survey to a remote science team. To confirm the accuracy of the automated identification program, the same spectra were manually inspected using The Spectral Geologist software, and visual assessments were conducted to interpret the mineral assemblage by relating the shape and wavelength of bands to known spectra, for example, those provided in an accompanying mineral library.

TSA uses a database of 500 samples of 42 SWIR active library (or “endmember”) minerals (Pontual, 1997), which are used to determine the closest match for unknown sample spectra. Similar databases have been developed for reflectance spectroscopy techniques by the U.S. Geological Survey (Clark *et al.*, 1990).

Reflectance spectra are often characterized by their albedo, which is the overall reflectance response of a sample (*i.e.*, dark samples have a low albedo). SWIR reflectance spectra display a spectral continuum that is shaped like an inverted hull. The continuum or “hull shape” may be relatively flat or significantly curved, depending upon the albedo of the specimen. Many software products, including TSA, provide a method for removal of the spectral continuum to improve the identification of spectral absorption bands. This normalization method, termed “convex hull removal” (Clark *et al.*, 1987), was applied to all of the spectra acquired in this study.

## RESULTS

This survey covered a 50- × 30-m section of outcrop at the Trendall Locality, an outcrop of the Strelley Pool Chert. To support the collection of spectra, 1,500 digital photographs were taken of the outcrop; these are available online at <http://aca.mq.edu.au/abrown.htm>. Figure 2 displays a geological map interpreted from these photos of the Trendall Locality.

A visual assessment was made of rock types at the Trendall locality before spectra were taken. This simulated the classification of rocks in the

TABLE 3. VISUALLY DETERMINED CHARACTERISTICS OF MINERALS AT TRENDALL OUTCROP

<i>Category name</i>	<i>Description</i>
Basalt	Overlying basaltic sequence, green-gray chlorite rich
Mudstone	Partially silicified layer with predominantly white clasts in microcrystalline gray chert, occasionally pure gray chert without visible clasts
Pebble conglomerate	Conglomeratic with clasts of black chert, some up to 2 cm across, with some fine white clasts in coarse-grained gray groundmass
Boulder conglomerate	Black microgranular quartz clasts with surficial red to purple iron staining
Black chert	Black microgranular quartz, smooth-textured, displaying conchoidal fracture, possibly kerogenous
Black and white chert	As for black chert, but with discontinuous bedding conformable white chert layers. Occurs in wide laminae and fine laminae forms
Quartz	Quartz vein, usually cutting through black chert layering. Textures commonly radiate in towards the center of veins and display chalcedonic texture typical of vug-filling quartz
Radiating crystal splays	Silicified, subvertical radiating crystal splays
Planar carbonate	Brown dolomite, roughly textured with fine grain size, planar layering evident with pervasive conical stromatolites
Siliceous planar laminate	As for carbonate layer, but dolomite partially replaced by silica. Color of unit varies from light brown to yellow, presumably varying with degree of silicification. Stromatolitic conical planar layering pervasive throughout the unit
Pyrophyllite schist	Pervasively altered unit, slight green in color and golden brown weathered schist. Quartz grains (relict amygdales) present. Occurs in bulbous (surrounded by white groundmass) and foliated forms

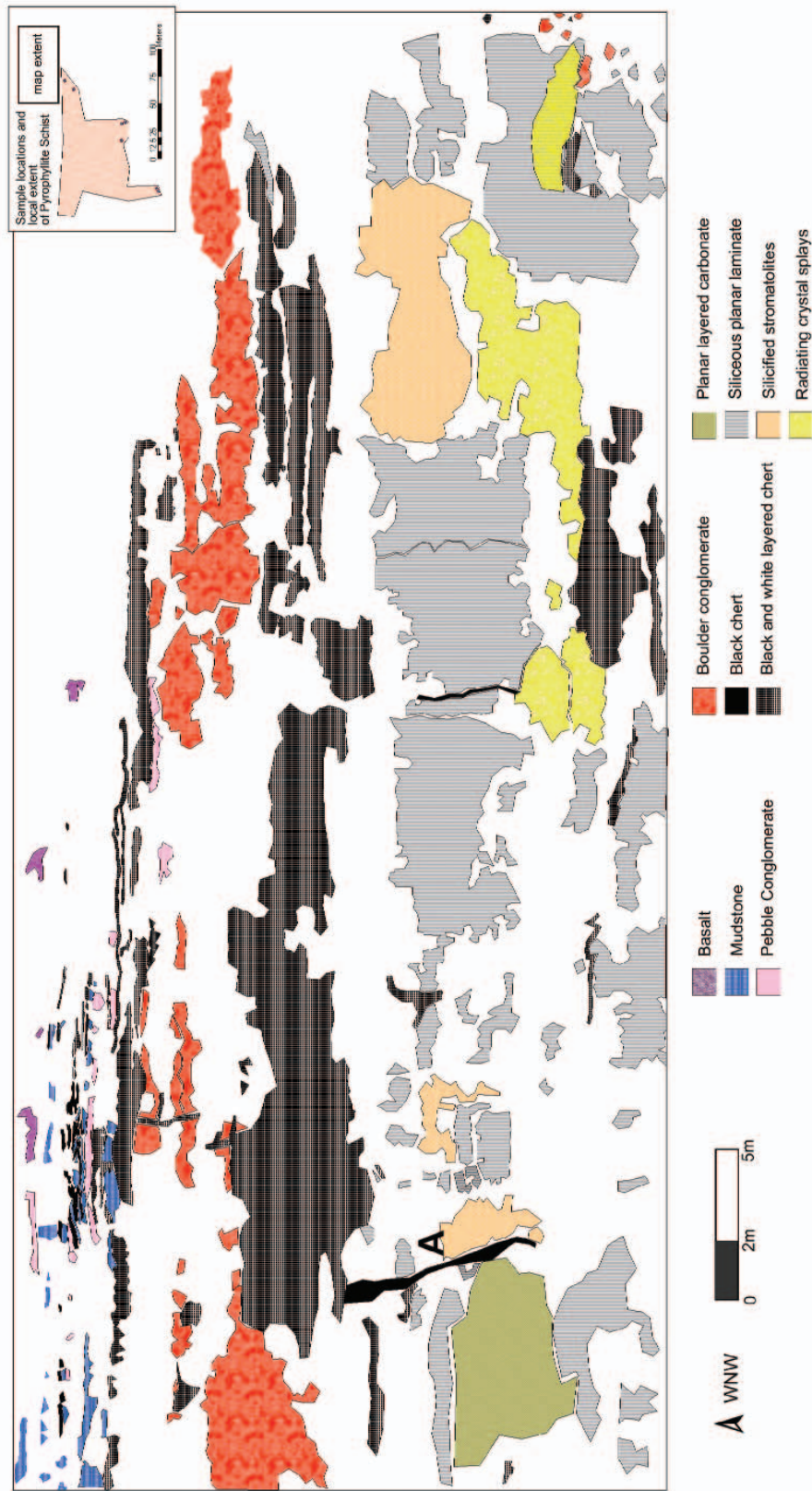


FIG. 2. Geological map of the Trendall Locality modified after Van Kranendonk and Hickman (2000) by using digital images of the outcrop.

vicinity of a robotic rover by remote scientists using panoramic images. Similar panoramic images were used intensively in NASA's Pathfinder (McSween *et al.*, 1999) and MER (Squyres *et al.*, 2003) missions. On the basis of this assessment, rocks were categorized according to color and texture, as indicated in Table 3. Examples of units present at the locality are shown in Fig. 3.

Following the rock type and unit categorization based on visual evidence, the area was surveyed with the PIMA spectrometer in the manner a rover might examine an outcrop. This was done by acquiring several spectra of each unit. At least seven spectra were acquired from each rock unit, sufficient to determine its spectral characteristics and identify any significant changes between spectra taken from the same unit.

The spectral features of each unit are discussed below. Apart from the overlying basalt unit and the underlying pyrophyllite schist unit, all units are part of the Strelley Pool Chert.

### *Basalt*

The overlying Euro Basalt is characterized by a light brown weathering rind and a green chlorite-rich mineral assemblage. It is fine grained and largely eroded at this location. Many samples are present as partially buried boulders rather than as competent outcrop.

The TSA analysis of the PIMA spectra of the basalt unit consistently identified Mg-chlorite within the unit (Table 4). An example spectrum is shown in Fig. 4. The chlorite was identified by its diagnostic absorption band centered at 2.25  $\mu\text{m}$ , lack of a feature at 1.55  $\mu\text{m}$  (typical of epidote), and the presence of associated chlorite features at 2.0 and 2.33  $\mu\text{m}$  (McLeod *et al.*, 1987).

### *Mudstone*

The mudstone unit is characterized by a gray fine-grained cherty groundmass, containing millimeter-sized white clasts that commonly display a sugary texture indicative of silicification. It lies near the top of the Trendall locality, among strata that have been classified as part of a clastic sequence based on previous research at this locality (Van Kranendonk and Hickman, 2000).

The spectra from the mudstone unit showed variable signatures, though most displayed a symmetric absorption band diagnostic of illite-muscovite at 2.2  $\mu\text{m}$ . The spectra also demonstrated variation in the amount of bound water,

characterized by differences in the shape of the absorption band at 1.91  $\mu\text{m}$ . Illite generally has a deeper absorption band at 1.91  $\mu\text{m}$  than muscovite. A typical spectrum of the mudstone unit is shown in Fig. 4. Visual interpretation of the mudstone spectra suggests a white mica is definitely present within the unit, a conclusion based on the regular appearance of the Al-OH absorption band at 2.2  $\mu\text{m}$ .

### *Pebble conglomerate*

The pebble conglomerate unit is characterized by a gray-green coarse-grained groundmass containing large (up to 2 cm) ovoid clasts. The clasts are often white and sometimes derived from underlying units, primarily black chert and mudstone. This unit is also part of the clastic succession at the Strelley Pool Chert (Van Kranendonk and Hickman, 2000). The presence of rip-up clasts of underlying units argues for a high-energy subaqueous depositional environment.

Since the conglomerate is constituted by clasts from the mudstone unit (among others), it is not surprising that the spectra of the pebble conglomerate unit were similar to those of the mudstone unit. It appeared, however, that the pebble conglomerate contained less water, an interpretation based on the presence of a weaker 1.9  $\mu\text{m}$  absorption band, and the fact that this band was characterized by a flatter hull shape. The unit was variably chloritized—strong chlorite absorption bands at 2.25 and 2.33  $\mu\text{m}$  were present in some samples, but absent in the majority of samples (Table 4).

### *Boulder conglomerate*

This unit consists of large (up to 5–10 cm) clasts, commonly of black chert, but also including black and white layered chert clasts and planar layered carbonate. The clasts often display red to purple staining due to the presence of iron oxides.

This unit displays overall low reflectance (typically <20%). Most spectra contained a water absorption band at 1.9  $\mu\text{m}$  that included bound water (centered at 1.915  $\mu\text{m}$ ) and unbound water (centered at 1.93  $\mu\text{m}$ ). Unbound water is typical of free, adsorbed, and trapped water (as expected for chert with  $\sim 1\%$  H<sub>2</sub>O), whereas bound water can be associated with minerals like illite and smectites (Aines and Rossman, 1994). Additional mineral absorptions of the spectra of this unit in-

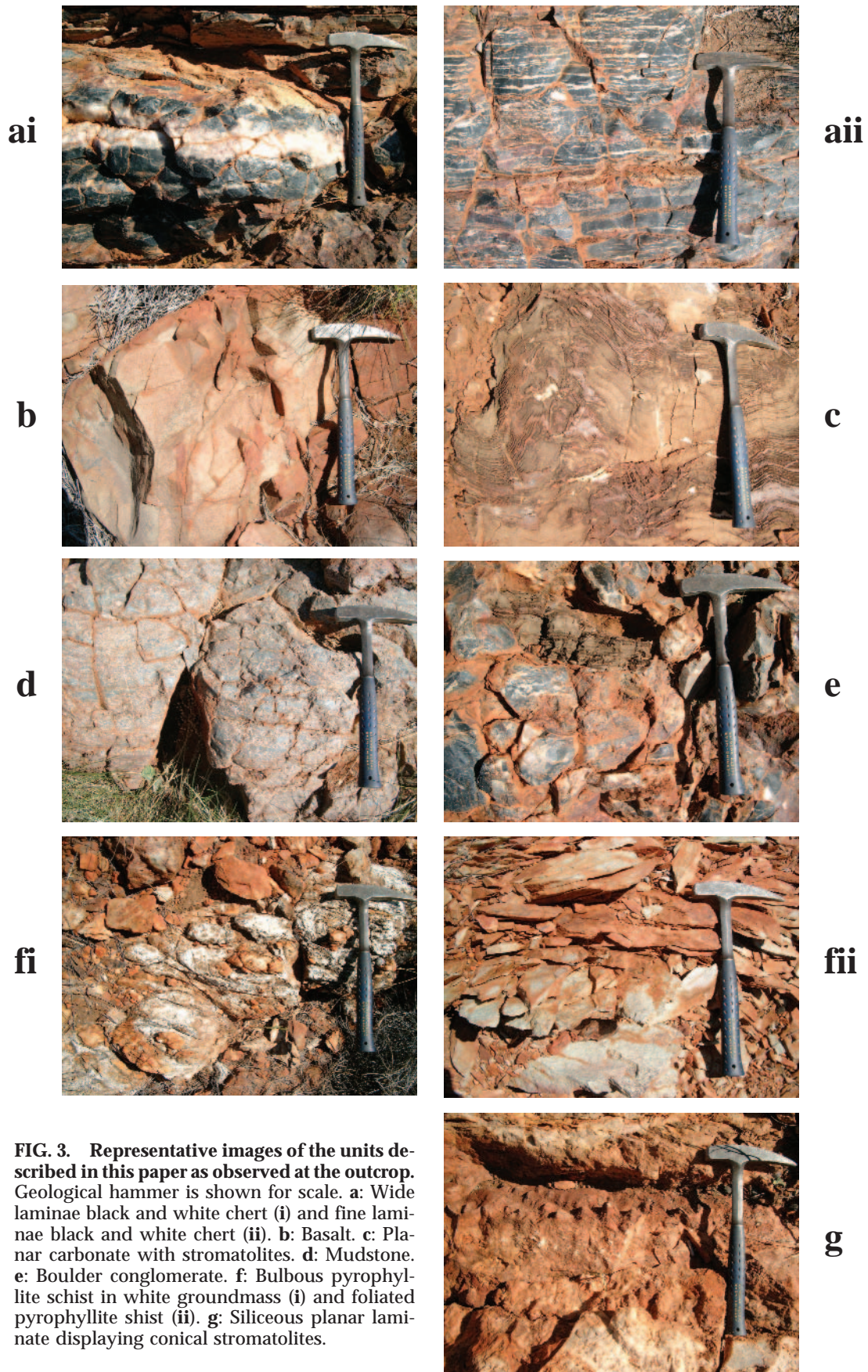


**FIG. 3.** Representative images of the units described in this paper as observed at the outcrop. Geological hammer is shown for scale. a: Wide laminae black and white chert (i) and fine laminae black and white chert (ii). b: Basalt. c: Planar carbonate with stromatolites. d: Mudstone. e: Boulder conglomerate. f: Bulbous pyrophyllite schist in white groundmass (i) and foliated pyrophyllite schist (ii). g: Siliceous planar laminate displaying conical stromatolites.

TABLE 4. MAP OF SPECTRAL VERSUS VISUAL CATEGORIES AT TRENDALL LOCALITY

Unit	SILICA	CARB	CARB	CARB	CARB	SULF	SULF	WMICA	WMICA	WMICA	CHLOR	CHLOR	MONT	KAOL	KAOL	KAOL	Total			
Basalt											3	8					11			
Mudstone						22	28							2			57			
Pebble conglomerate		1				7	12			2	1		1				27			
Boulder conglomerate	1							3									9			
Black chert						1	3			1							13			
Black and white chert	1		1					1									8			
Quartz	3											1					11			
Radiating crystal splays	2	1	1	2	1	1							2				13			
Planar carbonate	2	18	1	3										9	11		52			
Siliceous planar laminate	4				2	1	1							4	4	1	39			
Pyrophyllite schist																	13			
	Opal	Dolm	Magn	Sid	Ank	Calc	Na-Alu	K-Alu	Pyro	Musc	Ill	Fe-Chl	Int-Chl	Mg-Chl	Mont	Halloy	Kaol	Nac	Aspectral	253

All assessments were made automatically using TSA computer code. Mineral groups are abbreviated in uppercase and appear at the top of the table. See text for manual spectra identification and interpretation. SILICA = silica group, CARB = carbonate group, SULF = sulfate group, WMICA = white mica group, CHLOR = chlorite group, MONT = montmorillonite group, KAOL = kaolin group, Dolm = dolomite, Magn = magnesite, Sid = siderite, Ank = ankerite, Calc = calcite, K-Alu = potassium alumite, Na-Alu = sodium alumite, Pyro = pyrophyllite, Musc = muscovite, Ill = illite, Fe-Chl = iron-rich chlorite, Int-Chl = intermediate chlorite, Mg-Chl = clinocllore, Halloy = halloysite, Kaol = kaolinite, Nac = nacrite.

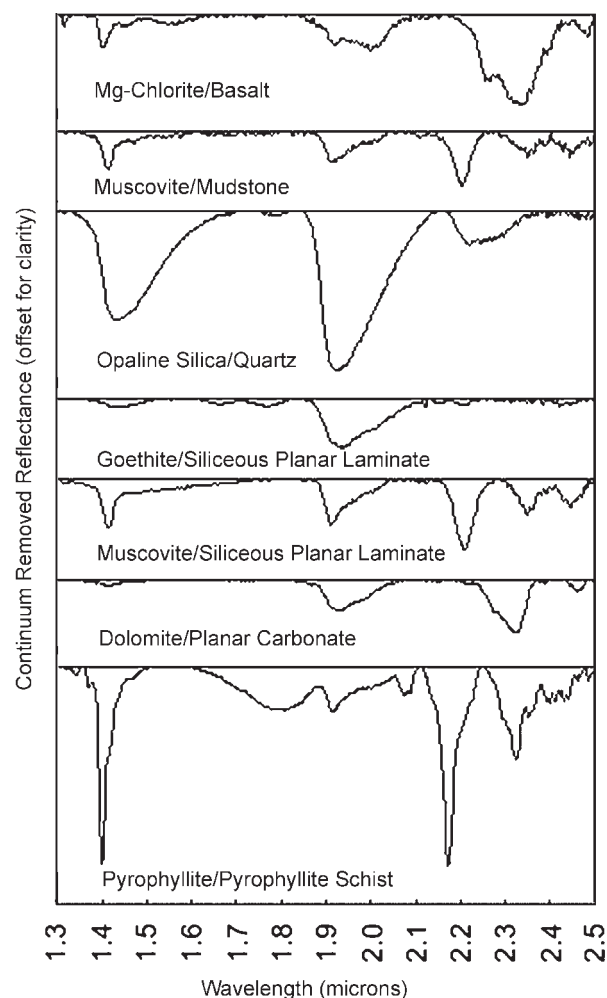


FIG. 4. Convex hull-removed example spectra of units found at the Trendall Locality.

cluded symmetric bands at  $2.2 \mu\text{m}$  due to the presence of illite-muscovite and coupled  $2.25$  and  $2.33 \mu\text{m}$  absorptions indicative of chlorite.

Since TSA could not identify any characteristics in spectra from this unit that contained black chert clasts, they were designated by the program as spectral (Table 4). That is not surprising given the fact that chert is inactive in the SWIR. TSA routine did identify opaline silica in one sample because of the presence of a broad Si-OH absorption band at  $2.215$ – $2.25 \mu\text{m}$ .

The presence of lithified planar laminate carbonate, black chert clasts, and quartz clasts within this conglomerate (see Fig. 3e) confirmed that it is older than the planar carbonate unit and that some of the black chert had been lithified prior to the deposition of this unit. The lack of planar siliceous clasts suggests that the silicification of the planar carbonate occurred after the conglomerate was formed.

### Black chert

The black chert unit consists of massive microgranular quartz. The black color is due to minor amounts of kerogen within the chert (Kato and Nakamura, 2003). At the Trendall Locality, massive black chert occurs typically as smooth, fine-grained quartz layers 5–10 cm thick when bedding conformable (often interleaved with other units, such as the mudstone unit), or as massive crosscutting veins 30–50 cm thick when oriented approximately normal to the stratigraphic layering. For the purposes of this study, the black chert laminations associated with white quartz layers were analyzed separately and grouped as the “black and white chert” unit (discussed below).

The PIMA spectra of the black chert unit were extremely dark (generally  $<10\%$  reflectance) and showed much weaker (if present) water and mineral absorption bands compared with the other units studied. TSA assigned a majority of the spectra as spectral (Table 4). The spectra displayed low signal-to-noise ratio because of their extremely low albedo. In low-albedo situations, the imposition of deviations due to instrument-related noise upon a small signal makes identification of absorption bands extremely difficult, even after convex hull removal.

### Black and white chert

The black and white chert unit is present in two forms (see Fig. 3a). The fine layered form is restricted to a relatively small area of the outcrop in the center of Fig. 2, and consists of microgranular black chert interstratified at a millimeter scale with microgranular white chert in parallel laminae that display flat bottoms and curved tops. The morphology of this unit suggests direct periodic sedimentary deposition in a quiet environment. The coarse layered form is laminar, and the width of laminae can range up to 5–10 cm. The wide laminae are subparallel to other units at the locality, and often appear to radiate from the vertical black dykes described previously. For this reason, the wide laminae black and white chert is likely a result of hydrothermal injection. Both forms of black and white layered chert display similar smooth microgranular texture. In most cases, the black chert surrounds the white chert. Both forms are generally found below the clastic upper units and above the carbonate and siliceous planar laminar units at the Trendall Locality.

The PIMA spectra of both forms of the black and white cherts could not be separated and are reported together here. The black and white chert showed higher albedo than the spectra of the black chert unit, though the water and mineral absorption bands were generally of similar relative intensity. TSA classified most of the spectra as aspectral (Table 4), even though absorptions at 2.2 and 2.3  $\mu\text{m}$  were apparent. These small features are most likely due to small amounts of white mica and carbonate.

### Quartz

Where quartz occurs in small (less than 4 cm wide) veins and displays irregular surface textures (unlike the smooth chert units), it was identified as a separate unit for the purposes of this study. The veins, which were not mapped, are not resolvable in Fig. 2 because of their small size. However, they all occurred within the black and white chert unit and in most cases represent vug-filling quartz that grew into cavities.

The PIMA spectra of these quartz veins showed a much stronger development of the unbound water absorption band centered at 1.93  $\mu\text{m}$ , as shown by a representative spectrum in Fig. 4. The broad and more defined character of this band contrasts with the weak and generally narrow bands due to bound water (*e.g.*, typical of the black cherts discussed previously). Some quartz spectra were very dark with albedos  $\sim 10\%$ , similar to those of the black cherts. A small number of the samples were identified by TSA as opaline silica (Table 4), based on the presence of an absorption band at 2.25  $\mu\text{m}$ . Some spectra showed symmetric Al-OH absorption bands, possibly related to illite-muscovite. However, most of the samples were classified by the TSA program as aspectral. The presence of opal is most likely due to late-stage weathering, evidenced by the sinuous, crosscutting, and vug-filling nature of the quartz veins.

### Radiating crystal splays

Radiating crystal splays were identified by earlier researchers (Van Kranendonk and Hickman, 2000) and were likened by them to beds of aragonite deposited in modern day travertine (see, *e.g.*, Jones *et al.*, 1997). Recent trace element studies suggest the unit represents a dolomitized replacement of radiating crystal fans, interpreted as secondary crystal growth below the sediment-water interface (Van Kranendonk *et al.*, 2003).

Although visibly silicified, the spectra of the unit identified dolomite within the unit because of the presence of a wide absorption band at 2.31  $\mu\text{m}$ .

### Planar layered carbonate

Planar laminated carbonate beds with pervasive conical stromatolites (Hofmann *et al.*, 1999) are present in the southeast part of the outcrop (bottom left of Fig. 2). At point A on Fig. 2, the unit is laterally crosscut by a subvertical black chert, which divides well-preserved planar laminated carbonate from the siliceous planar laminated unit.

The spectra of the planar layered dolomite displayed a bimodal nature (Fig. 5). Where stromatolite laminae had been preserved, the presence of Al-OH bonding indicative of kaolin was revealed by a deep asymmetric absorption at 2.2  $\mu\text{m}$ . This was accompanied by a relatively weak carbonate absorption band at 2.31  $\mu\text{m}$ . Where there was no preserved stromatolite laminae, the spectra lacked an absorption band at 2.2  $\mu\text{m}$  and displayed a relatively strong carbonate absorption at 2.31  $\mu\text{m}$ .

As shown in the graph in Fig. 5b, the antipathetic nature of the strength of the absorption bands at 2.2 and 2.31  $\mu\text{m}$  in the planar carbonate layer demonstrates that the presence of a kaolin mineral on the surface of the outcrop is obscuring the carbonate beneath it. The kaolin is most likely a weathering product or desert varnish caught in the closely spaced laminae following aeolian movement. This hypothesis was strengthened when the fresh underside of a hand sample was examined with the PIMA and found to be dolomite with no trace of kaolin, even on the preserved stromatolitic laminae, thus showing the kaolin was not an original part of the stromatolite laminae. This process of desert varnish trapping by stromatolitic laminae may be relevant on the windswept plains of Mars.

The nature of the weathering or varnish and its exclusive distribution on the exposed laminae that protrude beyond the pure carbonate is not entirely clear, but may provide one method for detecting preserved stromatolitic laminae in outcrops of martian rocks.

Beneath the planar layered carbonate lies a region devoid of stromatolite laminae. Irregular sinuous veins of quartz penetrate this region in a subvertical orientation, and terminate at a thin layer of black chert just below the lowest stromatolite laminae. The presence of unlaminated carbonate beneath the stromatolite layer suggests

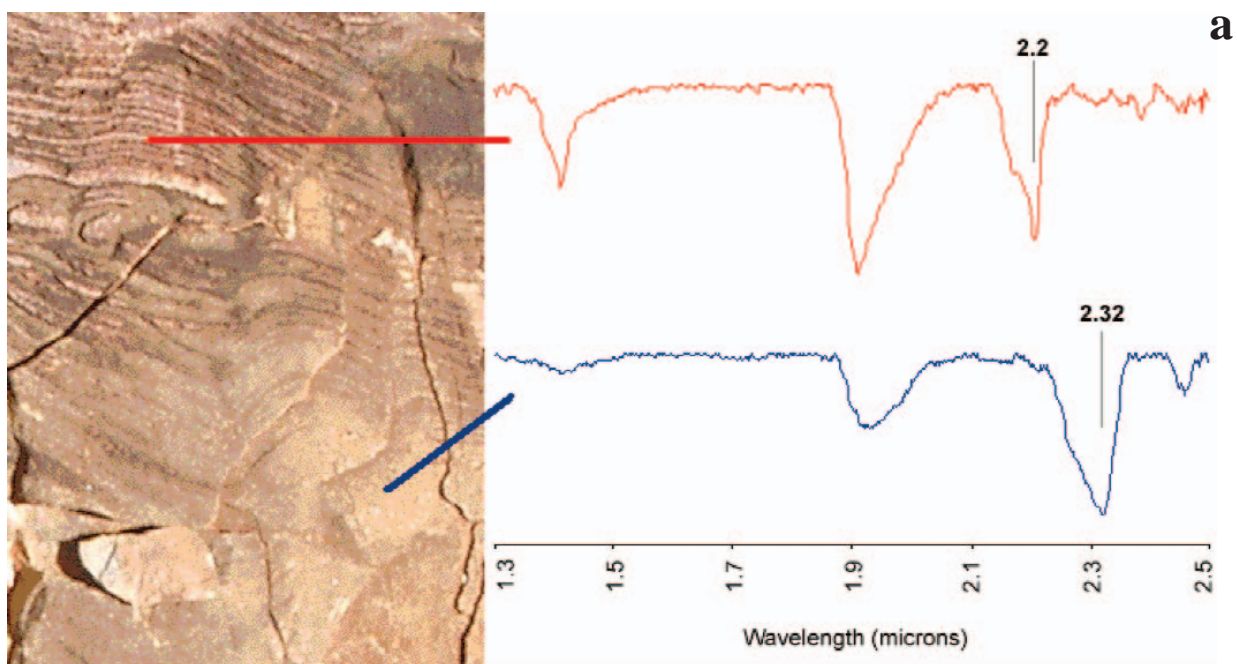
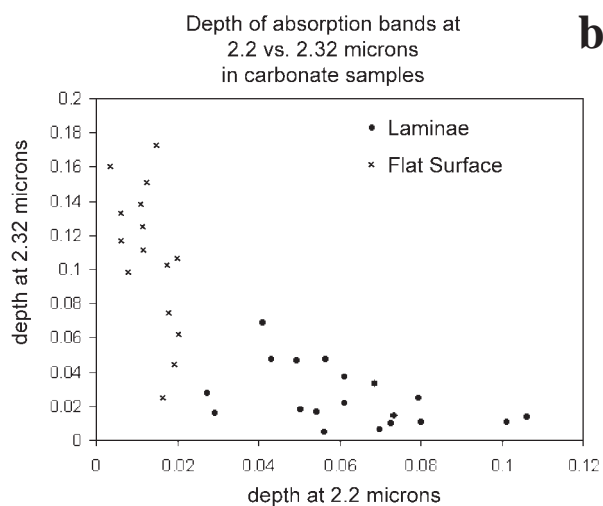


**FIG. 5. a:** Example spectra taken from preserved stromatolite laminae (above) and carbonate regions (below). **b:** Graph displaying antipathetic relationship of abundance of carbonate and kaolin within the planar carbonate region. See text for explanation.



carbonate deposition commenced prior to pervasive stromatolite growth. The origin of the quartz veins is not entirely clear, though they could be related to hydrothermal heating.

The radiating crystals region discussed earlier may be analogous to the unlaminated carbonate region due to their similar orientation (beneath the planar layered carbonate and siliceous units) and lack of stromatolitic features.

#### *Siliceous planar laminate*

This unit was visually assessed as the silicified portion of the planar carbonate layer based on the presence of stromatolitic laminae of similar verti-

cal and horizontal dimensions. The dominant color of the unit is dark gray to white. A smooth microcrystalline siliceous texture exists between the stromatolitic layers.

Horizontally, the siliceous planar laminate is separated from the planar carbonate regions by a vertical black chert dyke (point A on Fig. 2). The siliceous planar laminate also occurs above the carbonate planar unit, and is separated by a horizontal black chert dyke. The presence of the black dykes surrounding the carbonate layer suggests that the silicification process was impeded by the black chert that must have been in position before the silicification event occurred. Though the vertical black dykes at the Trendall

Locality may have been responsible for transportation of some hydrothermal fluids, such as those containing kerogen that contributed to the horizontal wide layered hydrothermal injection black and white cherts discussed earlier, it is unlikely that they were fluid conduits responsible for silicification of the planar layered carbonates, which was probably a later event.

The partially silicified nature of this carbonate unit was confirmed by the PIMA spectra, many of which showed minor absorption bands indicative of dolomite at  $2.31 \mu\text{m}$ . Several spectra contained an Al-OH related symmetric absorption band at  $2.2 \mu\text{m}$ , indicative of the presence of white mica. About half the spectra of this unit were designated by the TSA program as aspectral (Table 4).

Areas of intense red, brown, and yellow discoloration occur sporadically within the generally white siliceous unit. Several spectra from this region of the outcrop showed the distinctive bands of goethite at approximately  $1.65$  and  $1.75 \mu\text{m}$ . The sporadic nature of the discoloration suggests relatively recent weathering may be responsible for these features.

The PIMA spectra of the iron-oxide stained stromatolitic laminae showed weak evidence for kaolin with absorption bands centered at  $2.165$  and  $2.209 \mu\text{m}$ . Generally the spectra of the stromatolitic laminae were found to lack diagnostic absorption bands, but all displayed moderately high albedo.

#### *Pyrophyllite schist unit*

Stratigraphically beneath and to the south east of the area depicted in Fig. 2 lies a bleached brown to golden colored, heavily foliated schist that extends vertically for approximately  $50$  m beneath the Strelley Pool Chert. There is no outcrop at the contact between the chert and schist units. However, as the pyrophyllite schist unit converges on the base of the Strelley Pool Chert the alteration style changes from platy, foliated brown to golden outcrop to smaller bulbous outcrop surrounded by a white fine-grained groundmass (see Fig. 3f). The sample locations are shown in the inset of Fig. 2.

The spectra taken of the bulbous and foliated forms of the pyrophyllite schist unit clearly showed the presence of pyrophyllite, indicated by a diagnostic symmetric and sharp absorption band centered at  $2.165 \mu\text{m}$ , accompanied by a

smaller shoulder absorption band at  $2.195 \mu\text{m}$ . A representative example of this spectrum is shown in Fig. 4. Pyrophyllite is a typical alteration mineral resulting from acidic hydrothermal fluids rich in sulfur (high-sulfidation) (White and Hedenquist, 1990). No clear linkage has been established between the high-sulfidation alteration beneath the Strelley Pool Chert and the paragenesis of units within it. However, since no trace of pyrophyllite is found in the Euro basalt unit overlying the Strelley Pool Chert, it is likely that it formed prior to the pyrophyllite schist unit and acted as a barrier to the later high-sulfidation hydrothermal fluids. An alternative explanation is that the Strelley Pool Chert units were laid down on a partially eroded pyrophyllite schist unit, though no evidence for an unconformity has been reported between the units.

#### *Variation in octahedral Al of white mica*

Tschermak substitution in phyllosilicate minerals, where two Al atoms substitute for a Si atom and either a Fe or Mg atom in the crystal lattice  $[\text{Al}_2\text{Si}_{-1}(\text{Fe},\text{Mg})_1]$ , can be recognized in SWIR spectra by analysis of the Al-OH absorption band position at around  $2.2 \mu\text{m}$  (Duke, 1994). An increase in the Al content in a crystal structure containing Al-OH bonds is reflected by a decrease in the wavelength of the  $2.2 \mu\text{m}$  absorption band. The wavelength variations typically range from  $2.217$  to  $2.197 \mu\text{m}$ .

All units displaying the Al-OH absorption band around  $2.2 \mu\text{m}$  were analyzed for variations in the wavelength of the band minima. No significant Tschermak variations were found within the units at the Trendall Locality, though small variations were found between units. Table 5 summarizes the differences in average position of the Al-OH absorption bands within Al-OH bearing units.

The lack of Tschermak variation within units at the Trendall locality does not rule out variations in the same units some distance from this outcrop. These results suggest that at the scale of this outcrop, approximately  $50$  m across, there were no significant temperature variations that would have affected the abundance of Al within hydrothermal white mica.

#### *Geochemical analysis*

To support the PIMA mineral identification in the samples studied, x-ray diffraction (XRD) spectra were taken of selected samples from the Tren-

TABLE 5. VARIATIONS IN WAVELENGTH OF BAND MINIMA FOR AL-OH ABSORPTION BAND FOR AL-OH-BEARING UNITS AT THE TRENDALL LOCALITY

Unit	Al-OH band minima ( $\mu\text{m}$ )	Number of samples with Al-OH feature
Mudstone	2.207	52
Pebble conglomerate	2.205	23
Planar carbonate	2.207	20
Siliceous planar laminate	2.209	10
Pyrophyllite	2.197	11

dall locality. Because of the historical importance and current state of preservation of the site, sampling is discouraged by the Geological Survey of Western Australia, and so only limited sampling was undertaken. Rietveld analysis (Rietveld, 1969) was carried out by Sietronics Pty Ltd. (Canberra, ACT, Australia) using a Bruker AXS D4 x-ray diffractometer, and all other samples were run at CSIRO Exploration and Mining using a Phillips PW 1050 diffractometer using CuK  $\alpha$  radiation. Each run was conducted with the x-ray diffractometer set to the following levels: 40 kV, 40 mA, step size of  $0.03^\circ$ , and count time per step of 1.8 s.

Two samples of the planar carbonate unit were analyzed. The results (Fig. 6) showed the presence of quartz and dolomite. No other minerals were detected. Rietveld analysis was carried out on one of the samples using the Siroquant program (Taylor, 1991), which indicated that the sample contained 45 wt% quartz and 55 wt% dolomite. The XRD analysis supported the SWIR detection of dolomite in the planar carbonate unit. One sample of the pyrophyllite schist unit was analyzed, and pyrophyllite and quartz were identified. Quartz was identified as the sole min-

eral component in samples of the black and white chert, mudstone, and silicified chert.

## DISCUSSION

Previous studies have demonstrated the ability of SWIR techniques to map alteration minerals in hydrothermally altered terrain (see, e.g., Thompson *et al.*, 1999). This study has shown the utility of using a SWIR instrument to identify mineral phases indicative of hydrothermal alteration in a hydrothermally altered, silicified, stromatolitic carbonate and clastic succession.

Highly silicified environments are typical of Archean greenstone terrains that have undergone moderate hydrothermal alteration (Gibson *et al.*, 1983; Duchac and Hanor, 1987; Van Kranendonk and Pirajno, 2004). Archean greenstone terrains often contain cherts that preserve textures and fabrics indicative of past biological activity such as stromatolites (De Wit *et al.*, 1982). Some workers have indicated that chert deposits may be ideal places to search for fossilized life on Mars (Walter and Des Marais, 1993).

### *Similarities between hydrothermal events in the Pilbara and Mars*

It has been postulated that impact craters (Newson *et al.*, 2001) and sites of gully formation (Brakenridge *et al.*, 1985; Gulick, 1998) may be sites on Mars where hydrothermal waters may have penetrated the martian regolith. Sites of hydrothermal activity on Mars may be characterized by silicification and cherty sediments such as those found at the Trendall Locality. Such deposits would be ideal sites for the preservation of microbial mat fabrics (Walter and Des Marais, 1993).

Although SWIR instruments are limited in their ability to examine low-albedo black cherts, we have shown that the SWIR technique can identify minerals such as carbonates and phyl-

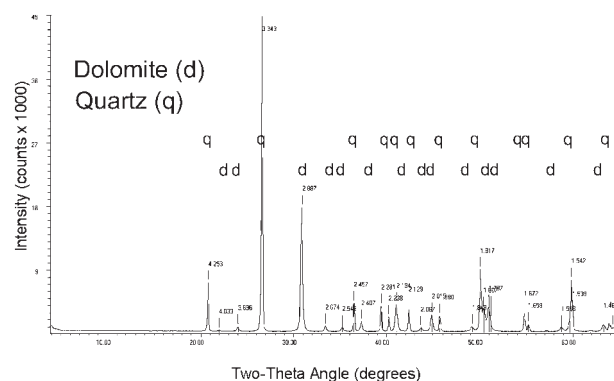


FIG. 6. XRD spectra of the stromatolitic carbonate unit, showing peaks for dolomite.

losilicates and be used to characterize the degree and nature of alteration of such minerals, a critical precursor to the localization and discovery of life or preserved fossils. In the course of a typical rover mission on Mars, and particularly if a rover were to encounter a site of astrobiological interest on Mars, the minerals present at the site would need to be quickly surveyed to localize areas where further, more time-consuming analyses could be carried out. A SWIR instrument such as the PIMA could serve this role for a rover operating in such a reconnaissance mode.

In preparation for the 2003 Mars Exploration Rover missions, NASA science and engineering teams used an instrument called IPS, which is similar to PIMA, on its evaluation rovers (Haldemann *et al.*, 2002). This instrument differs from PIMA in that the instrument does not have to be in contact with the rock in order to obtain a spectrum. The light of the sun is used by IPS as an illumination source. The instrument was found to add considerably to the geologists' ability to characterize mineralogically distinct geological sequences in a rover-remote science team scenario (Jolliff *et al.*, 2002).

This study shows that automatic rock classification using an SWIR reflectance spectroscopy instrument such as PIMA (Pedersen *et al.*, 1999; Moody *et al.*, 2001; Gulick *et al.*, 2003) would prove useful in future extraterrestrial robotic missions. Mineral identification algorithms such as those used by TSA may prove useful in such a system, though this study has highlighted the difficulty of automatic recognition of low-albedo reflectance spectra (such as those of black cherts), due to low achievable signal-to-noise ratio.

The ability of the PIMA to identify mineral modes makes it ideal to support elemental abundance instruments such as the Alpha Proton X-ray Spectrometer (Golombek, 1998) or Laser Induced Breakdown Spectrometer (Wiens *et al.*, 2002). The minerals modes provided by a PIMA spectrum could be quantified using a standard normalization technique when combined with an elemental abundance measurement. Unusual hydroxyl-bearing mineral assemblages, such as jarosite and saponite, can be detected unambiguously by the PIMA.

## CONCLUSIONS

This study has demonstrated the ability of SWIR reflectance spectroscopy to identify miner-

als in an Archean hydrothermally altered environment. Minerals identified included carbonates such as dolomite, white micas such as illite-muscovite, opaline silica, clays, and chlorite. These identifications supplemented visual assessments and aided in the geological interpretation of the outcrop under study.

The SWIR spectroscopic method is ideal for mounting on a small rover for remote field analysis of collected samples. It is lightweight and has low power requirements, being able to be operated with a 12-V battery. With an instrument such as the PIMA, calibration and spectrum collection can be completed in around 2 min. The availability of a large body of research and spectral libraries coupled with advanced algorithms in packages such as TSA make the technique a low-risk supplementary and reconnaissance instrument suitable for mineral detection of samples that require virtually no sample preparation. We have demonstrated its utility even in highly silicified environments.

The results of this study show that SWIR spectroscopy contributed to the classification and interpretation of the geology of the Strelley Pool Chert. New observations made using the PIMA instrument contributed the following information:

1. The presence and extent of carbonate and partially replaced dolomitic carbonate was confirmed.
2. Preserved stromatolitic laminae at the Trendall Locality are covered by a kaolin-rich desert varnish, most probably trapped by the stromatolitic laminae, in contrast to the purely dolomitic nature of the carbonate groundmass.
3. Pyrophyllite was detected in an extensively altered and foliated unit (pyrophyllite schist) beneath the silicified outcrop, which suggests that acidic, high-sulfidation hydrothermal alteration has taken place directly beneath the Strelley Pool Chert.

## ACKNOWLEDGMENTS

This research would not have been possible without the generous assistance of the Geological Survey of Western Australia. Assistance in the field from Naomi Mathers was greatly appreciated. Assistance with XRD analysis from Michael

Verrall, CSIRO, was appreciated. Reviews from Martin Van Kranendonk, Kai Yang, and Sherry Cady were helpful and enlightening and produced a much-improved manuscript. Abigail Allwood is thanked for her comments on the manuscript. CSIRO Division of Exploration and Mining is thanked for the loan of its PIMA II field spectrometer. Jonathon Huntington and Peter Mason at CSIRO are thanked for their assistance with processing and interpretation of SWIR spectra.

## ABBREVIATIONS

PIMA, Portable Infrared Mineral Analyser; REE, Rare Earth Element; SWIR, short-wave infrared; TSA, The Spectral Analyst; XRD, x-ray diffraction.

## REFERENCES

- Aines, R.D. and Rossman, G.R. (1984) Water in mineral? A peak in the infrared. *J. Geophys. Res.* 89, 4059–4071.
- Awramik, S.M., Schopf, J.W., and Walter, M.R. (1983) Filamentous fossil bacteria from the Archaean of Western Australia. *Precambrian Res.* 20, 357–374.
- Baird, A.K. and Clark, B.C. (1981) On the original igneous source of martian fines. *Icarus* 45, 113–123.
- Barley, M.E. (1984) Volcanism and hydrothermal alteration, Warrawoona Group, East Pilbara. In *Archean and Proterozoic Basins of the Pilbara, Western Australia*, edited by J.R. Muhling, D.I. Groves, and T.S. Blake, Geology Department (Key Centre) and University Extension, The University of Western Australia, Perth, pp. 23–26.
- Bierwirth, P., Huston, D., and Blewett, R. (2002) Hyperspectral mapping of mineral assemblages associated with gold mineralization in the Central Pilbara, Western Australia. *Econ. Geol.* 97, 819–826.
- Blaney, D.L. (2002) Visible to short wavelength infrared spectroscopy on rovers: Why we need it on Mars and what we need to do on Earth. In *LPI Contribution No. 1148: Workshop on Mars Infrared Spectroscopy: From Theory and the Laboratory to Field Observations*, edited by L. Kirkland, J. Mustard, J. McAfee, B. Hapke, and M. Ramsey, Lunar and Planetary Institute, Houston, p. 2010.
- Blewett, R.S., Shevchenko, S., and Bell, B. (2004) The North Pole Dome: A non-diapiric dome in the Archaean Pilbara Craton, Western Australia. *Precambrian Res.* 133, 105–120.
- Brakenridge, G.R., Newsom, H.E., and Baker, V.R. (1985) Ancient hot springs on Mars: Origins and paleoenvironmental significance of small Martian valleys. *Geology* 13, 859–862.
- Brown, A.J. (2003) Hyperspectral mapping of an ancient hydrothermal system [abstract # 12979]. *Astrobiology* 2, 635.
- Buick, R. (1990) Microfossil recognition in Archean rocks: An appraisal of spheroids and filaments from a 3500 m.y. old chert-barite unit at North Pole, Western Australia. *Palaios* 5, 441–459.
- Buick, R. and Dunlop, J.S.R. (1990) Evaporitic sediments of early Archean age from the Warrawoona Group, North Pole, Western Australia. *Sedimentology* 37, 247–277.
- Christensen, P.R., Bandfield, J.L., Smith, M.D., Hamilton, V.E., and Clark, R.N. (2000) Identification of a basaltic component on the Martian surface from Thermal Emission Spectrometer data. *J. Geophys. Res. Planets* 105(E4), 9609–9621.
- Clark, R.N., King, T.V.V., and Gorelick, N. (1987) Automatic continuum analysis of reflectance spectra. In *JPL Publication 87-30: Proceedings of the Third Airborne Imaging Spectrometer Data Analysis Workshop*, Jet Propulsion Laboratory, Pasadena, CA, pp. 138–142.
- Clark, R.N., King, T.V.V., Klejwa, M., and Swayze, G.A. (1990) High spectral resolution reflectance spectroscopy of minerals. *J. Geophys. Res.* 95(B), 12653–12680.
- Cudahy, T.J., Okada, K., and Brauhart, C. (2000) Targeting VMS-style Zn mineralization at Panorama, Australia, using airborne hyperspectral VNIR-SWIR HyMap data. In *International Conference on Applied Geologic Remote Sensing, 14th Las Vegas, Nevada, Proceedings*, Environmental Research Institute of Michigan, Las Vegas, pp. 395–402.
- De Wit, M.J., Hart, R., Martin, A., and Abbott, P. (1982) Archean abiogenic and probable biogenic structures associated with mineralized hydrothermal vent systems and regional metasomatism, with implications for greenstone belt studies. *Econ. Geol.* 77, 1783–1802.
- Deer, W.A., Howie, R.A., and Zussman, J. (1992) *An Introduction to the Rock Forming Minerals*, Longman, Harlow, UK.
- Duchac, K.C. and Hanor, J.S. (1987) Origin and timing of the metasomatic silicification of an early Archean komatiite sequence, Barberton Mountain Land, South Africa. *Precambrian Res.* 37, 125–146.
- Duke, E.F. (1994) Near infrared spectra of muscovite, Tschermak substitution, and metamorphic reaction progress: Implications for remote sensing. *Geology* 22, 621–624.
- Dunlop, J.S.R., Muir, M.D., Milne, V.A., and Groves, D.I. (1978) A new microfossil assemblage from the Archaean of Western Australia. *Nature* 274, 676–678.
- Gaffey, S.J. (1986) Spectral reflectance of carbonate minerals in the visible and near infrared (0.35–2.55 microns): Calcite aragonite and dolomite. *Am. Mineral.* 71, 151–162.
- Galley, A.G. (1993) Characteristics of semi-conformable alteration zones associated with volcanogenic massive sulfide districts. *J. Geochem. Explor.* 48, 175–200.
- Gibson, H.L., Watkinson, D.H., and Comba, C.D.A. (1983) Silicification: Hydrothermal alteration in an Archean geothermal system within the Amulet Rhyolite Formation, Noranda, Quebec. *Econ. Geol.* 78, 954–971.
- Golombek, M.P. (1998) The Mars Pathfinder mission. *Sci. Am.* 279(1), 40–49.

- Groves, D.I., Dunlop, J.S.R., and Buick, R. (1981) An early habitat of life. *Sci. Am.* 245(4), 56–65.
- Gulick, V.C. (1998) Magmatic intrusions and a hydrothermal origin for fluvial valleys on Mars. *J. Geophys. Res. Planets* 103(E8), 19365–19387.
- Gulick, V.C., Morris, R.L., Gazis, P., Bishop, J.L., Alena, R., Hart, S.D., and Horton, A. (2003) Automated rock identification for future Mars exploration missions [abstract 2103]. In *34<sup>th</sup> Lunar and Planetary Science Conference Abstracts*, LPI Contribution No. 1156, Lunar and Planetary Institute, Houston.
- Haldemann, A.F.C., Baumgartner, E.T., Bearman, G.H., Blaney, D.L., Brown, D.I., Dolgin, B.P., Dorsky, L.I., Huntsberger, T.L., Ksendzov, A., Mahoney, J.C., McKelvey, M.J., Pavri, B.E., Post, G.A., Tubbs, E.F., Arvidson, R.E., Snider, N.O., Squyres, S.W., Gorevan, S., Klingelhofer, G., Bernhardt, B., and Gellert, R. (2002) FIDO science payload simulating the Athena Payload. *J. Geophys. Res. Planets* 107(E11), article number 8006.
- Herrmann, W., Blake, M., Doyle, M., Huston, D., Kamprad, J., Merry, N., and Pontual, S. (2001) Short wavelength infrared (SWIR) spectral analysis of hydrothermal alteration zones associated with base metal sulfide deposits at Rosebery and Western Tharsis, Tasmania, and Highway-Reward, Queensland. *Econ. Geol.* 96, 939–955.
- Hofmann, H.J., Grey, K., Hickman, A.H., and Thorpe, R.I. (1999) Origin of 3.45 Ga coniform stromatolites in Warrawoona Group, Western Australia. *GSA Bull.* 111, 1256–1262.
- Hunt, G.R. (1979) Near infrared (1.3–2.4  $\mu\text{m}$ ) spectra of alteration minerals—potential for use in remote sensing. *Geophysics* 44, 1974–1986.
- Huston, D., Kamprad, J., and Brauhart, C. (1999) Definition of high-temperature alteration zones with PIMA: An example from the Panorama VHMS district, central Pilbara Craton. *AGSO Res. Newslett.* 30, 10–12.
- Jolliff, B., Knoll, A., Morris, R.V., Moersch, J., McSween, H., Gilmore, M., Arvidson, R., Greeley, R., Herkenhoff, K., and Squyres, S. (2002) Remotely sensed geology from lander-based to orbital perspectives: Results of FIDO rover May 2000 field tests. *J. Geophys. Res. Planets* 107(E11), article number 8008.
- Jones, B., Renaut, R.W., and Rosen, M.R. (1997) Vertical zonation of biota in microstromatolites associated with hot springs, North Island, New Zealand. *Palaios* 12, 220–236.
- Kato, Y. and Nakamura, K. (2003) Origin and global tectonic significance of Early Archean cherts from the Marble Bar greenstone belt, Pilbara Craton, Western Australia. *Precambrian Res.* 125, 191–243.
- Kitajima, K., Maruyama, S., Utsunomiya, S., and Liou, J.G. (2001) Seafloor hydrothermal alteration at an Archean mid-ocean ridge. *J. Metamorph. Geol.* 19, 581–597.
- Lindsay, J.F., Brasier, M.D., McLoughlin, N., Green, O.R., Fogel, M., McNamara, K.M., Steele, A., and Mertzman, S.A. (2003) Abiotic Earth—establishing a baseline for earliest life, data from the Archean of Western Australia [abstract 1137]. In *34<sup>th</sup> Lunar and Planetary Science Conference Abstracts*, LPI Contribution No. 1156, Lunar and Planetary Institute, Houston.
- Lowe, D.R. (1983) Restricted shallow-water sedimentation of early Archean stromatolitic and evaporitic strata of the Strelley Pool Chert, Pilbara Block, Western Australia. *Precambrian Res.* 19, 239–283.
- McLeod, R.L., Gabell, A.R., Green, A.A., and Gardavski, V. (1987) Chlorite infrared spectral data as proximity indicators of volcanogenic massive sulfide mineralization. In *Pacific Rim Congress 87, Gold Coast, 1987, Proceedings*, Australasian Institute of Mining and Metallurgy, Parkville, Australia, pp. 321–324.
- McSween, H.Y., Murchie, S.L., Crisp, J.A., Bridges, N.T., Anderson, R.C., Bell, J.F., Britt, D.T., Bruckner, J., Dreibus, G., Economou, T., Ghosh, A., Golombek, M.P., Greenwood, J.P., Johnson, J.R., Moore, H.J., Morris, R.V., Parker, T.J., Rieder, R., Singer, R., and Wanke, H. (1999) Chemical, multispectral, and textural constraints on the composition and origin of rocks at the Mars Pathfinder landing site. *J. Geophys. Res. Planets* 104(E4), 8679–8715.
- Meyer, C. and Hemley, J.J. (1967) Wallrock alteration. In *Geochemistry of Hydrothermal Ore Deposits*, edited by H.L. Barnes, Holt, Rinehart and Wilson, New York, pp. 166–235.
- Moody, J., Silva, R., and Vanderwaart, J. (2001) Data filtering for automatic classification of rocks from reflectance spectra. In *Seventh ACM SIGKIDD International Conference on Knowledge Discovery and Data Mining*, ACM, San Francisco, pp. 347–352.
- Mustard, J.F. and Sunshine, J.M. (1995) Seeing through the dust—martian crustal heterogeneity and links to the SNC meteorites. *Science* 267, 1623–1626.
- Newsom, H.E., Hagerty, J.J., and Thorsos, I.E. (2001) Location and sampling of aqueous and hydrothermal deposits in martian impact craters. *Astrobiology* 1, 71–88.
- Pedersen, L., Apostolopoulos, D., Whittaker, W., Cassidy, W., Lee, P., and Roush, T. (1999) Robotic rock classification using visible light reflectance spectroscopy: Preliminary results from the Robotic Antarctic Meteorite Search program [abstract 1340]. In *30<sup>th</sup> Lunar and Planetary Science Conference Abstracts*, LPI Contribution No. 964, Lunar and Planetary Institute, Houston.
- Pontual, S. (1997) *G-Mex Vol. 1: Special Interpretation Field Manual*, Ausspec International, Pty Ltd., Kew, Australia.
- Reed, M.H. (1983) Seawater-basalt reaction and the origin of greenstones and related ore deposits. *Econ. Geol.* 78, 466–485.
- Reyes, D.P. and Christensen, P.R. (1994) Evidence for komatiite-type lavas on Mars from Phobos Ism data and other observations. *Geophys. Res. Lett.* 21, 887–890.
- Rietveld, H.M. (1969) A profile refinement method for nuclear and magnetic structures. *J. Appl. Crystallogr.* 2, 65–71.
- Schopf, J.W. (1993) Microfossils of the Early Archean Apex Chert: New evidence of the antiquity of life. *Science* 260, 640–646.
- Squyres, S.W., Arvidson, R.E., Baumgartner, E.I., Bell, J.F., Christensen, P.R., Gorevan, S., Herkenhoff, K.E., Klingelhofer, G., Madsen, M.B., Morris, R.V., Rieder, R., and Romero, R.A. (2003) Athena Mars rover science investigation. *J. Geophys. Res.* 108, article number 8062.

- Taylor, J.C. (1991) Computer programs for standardless quantitative analysis of minerals using the full powder diffraction profile. *Powder Diffract.* 6, 2–9.
- Thomas, M. and Walter, M.R. (2002) Application of hyperspectral infrared analysis of hydrothermal alteration on Earth and Mars. *Astrobiology* 2, 335–351.
- Thompson, A.J.B. and Thompson, J.F.H. (1996) *Atlas of Alteration: A Field and Petrographic Guide to Hydrothermal Alteration Minerals*, Mineral Deposits Division, Geological Association of Canada, St. John's, Newfoundland.
- Thompson, A.J.B., Hauff, P.L., and Robitaille, A.J. (1999) Alteration mapping in exploration: Application of short-wave infrared (SWIR) spectroscopy. *SEG Newslett.* 39, 16–27.
- Thorpe, R.I., Hickman, A.H., Davis, D.W., Mortensen, J.K., and Trendall, A.F. (1992) U-Pb zircon geochronology of Archaean felsic units in the Marble Bar region, Pilbara Craton, Western Australia. *Precambrian Res.* 56, 169–189.
- Ueno, Y. (1998) Earth's oldest bacteria (3.5 Ga) from W. Australia and the carbon isotope signature [abstract]. *GSA Abstracts Programs* 30, A-98.
- Ueno, Y., Isozaki, Y., Yurimoto, H., and Maruyama, S. (2001a) Carbon isotopic signatures of individual microfossils(?) from Western Australia. *Int. Geol. Rev.* 43, 196–212.
- Ueno, Y., Maruyama, S., Isozaki, Y., and Yurimoto, H. (2001b) Early Archaean (ca. 3.5 Ga) microfossils and <sup>13</sup>C depleted carbonaceous matter in the North Pole area, Western Australia: Field occurrence and geochemistry. In *Geochemistry and the Origin of Life*, edited by S. Nakashima, S. Maruyama, A. Brack, and B.F. Windley, Universal Academy Press, Tokyo, pp. 203–236.
- Van Kranendonk, M.J. (2000) *Geology of the North Shaw 1:100 000 Sheet*, Geological Survey of Western Australia, Department of Minerals and Energy, Perth.
- Van Kranendonk, M. and Hickman, A.H. (2000) *Archaean Geology of the North Shaw Region, East Pilbara Granite Greenstone Terrain, Western Australia—A Field Guide*, Geological Survey of Western Australia, Department of Minerals and Energy, Perth.
- Van Kranendonk, M.J. and Pirajno, F. (2004) Geochemistry of metabasalts and hydrothermal alteration zones associated with ca. 3.45 Ga chert +/- barite deposits: Implications for the geological setting of the Warrawoona Group, Pilbara Craton, Australia. *Geochem. Explor. Environ. Anal.* 4, 253–278.
- Van Kranendonk, M., Webb, G.E., and Kamber, B.S. (2003) Geological and trace element evidence for a marine sedimentary environment of deposition and biogenicity of 3.45 Ga stromatolitic carbonates in the Pilbara Craton, and support for a reducing Archaean ocean. *Geobiology* 1, 91–108.
- Walter, M.R. and Des Marais, D.J. (1993) Preservation of biological information in thermal-spring deposits—developing a strategy for the search for fossil life on Mars. *Icarus* 101, 129–143.
- Walter, M.R., Buick, R., and Dunlop, J.S.R. (1980) Stromatolites 3400–3500 Myr old from the North Pole area, Western Australia. *Nature* 284, 443–445.
- White, N.C. and Hedenquist, J.W. (1990) Epithermal environments and styles of mineralization: variations and their causes, and guideline for exploration. *J. Geochem. Explor.* 36, 445–474.
- Wiens, R.C., Arvidson, R.E., Cremers, D.A., Ferris, M.J., Blacic, J.D., Seelos, F.P., and Deal, K.S. (2002) Combined remote mineralogical and elemental identification from rovers: Field and laboratory tests using reflectance and laser-induced breakdown spectroscopy. *J. Geophys. Res. Planets* 107(E11), article number 8004.
- Yang, K., Huntington, J.F., Brown, P.R.L., and Ma, C. (2000) An infrared spectral reflectance study of hydrothermal alteration minerals from the Te Mihi sector of the Wairakei geothermal system, New Zealand. *Geothermics* 29, 377–392.
- Yang, K., Browne, P.R.L., Huntington, J.F., and Walshe, J.L. (2001) Characterising the hydrothermal alteration of the Broadlands-Ohaaki geothermal system, New Zealand, using short-wave infrared spectroscopy. *J. Volcanol. Geotherm. Res.* 106, 53–65.

Address reprint requests to:

Adrian Brown  
 Australian Centre for Astrobiology  
 Macquarie University  
 North Ryde, NSW 2109, Australia

E-mail: abrown@els.mq.edu.au